

## Tunable electrical and optical properties of hafnium nitride thin films

I. L. Farrell,<sup>1,2</sup> R. J. Reeves,<sup>1,2</sup> A. R. H. Preston,<sup>2,3</sup> B. M. Ludbrook,<sup>2,3</sup> J. E. Downes,<sup>4</sup> B. J. Ruck,<sup>2,3,a)</sup> and S. M. Durbin<sup>2,5</sup>

<sup>1</sup>Department of Physics and Astronomy, University of Canterbury, Christchurch 8140, New Zealand

<sup>2</sup>The MacDiarmid Institute for Advanced Materials and Nanotechnology, New Zealand

<sup>3</sup>School of Chemical and Physical Sciences, Victoria University, P.O. Box 600, Wellington 6140, New Zealand

<sup>4</sup>Department of Physics and Engineering, Macquarie University, New South Wales 2109, Australia

<sup>5</sup>Department of Electrical and Computer Engineering, University of Canterbury, Christchurch 8140, New Zealand

(Received 11 November 2009; accepted 27 January 2010; published online 19 February 2010)

We report structural and electronic properties of epitaxial hafnium nitride films grown on MgO by plasma-assisted pulsed laser deposition. The electronic structure measured using soft x-ray absorption and emission spectroscopy is in excellent agreement with the results of a band structure calculation. We show that by varying the growth conditions we can extend the films' reflectance further toward the UV, and we relate this observation to the electronic structure. © 2010 American Institute of Physics. [doi:10.1063/1.3327329]

Metal nitrides are fascinating and technologically important materials, variously exhibiting metallic, semiconducting, or magnetic properties. They are increasingly used in electronic devices, and from a fundamental viewpoint they can serve as excellent testing grounds for advanced electronic structure calculations.<sup>1–5</sup> Recently, hafnium nitride (HfN) has attracted attention, particularly as a buffer layer to enable epitaxial growth of GaN on Si.<sup>6,7</sup> It has good diffusion resistance, and most importantly its metallic nature provides a high reflectivity<sup>8</sup> that can be utilized as a back contact to enhance light extraction from optical devices. HfN<sub>x</sub> also shows potential for use as a field effect transistor metal gate, where varying the nitrogen content allows the work function to be tailored over the entire range from the silicon valence to conduction band edges.<sup>9</sup>

It is known that the lattice constant and electrical conductivity of HfN are dependent on the stoichiometry,<sup>10,11</sup> and a recent theoretical study has examined the defect structure by which the nonstoichiometry is accommodated in HfN<sub>1-x</sub>.<sup>12</sup> However, no experimental studies have addressed the full electronic band structure, nor have the effects of changes in stoichiometry or crystallinity on the electronic structure been reported. Here, we use x-ray spectroscopy data obtained from epitaxial HfN films to verify a band structure calculation, and we use this band structure to interpret optical reflectance data obtained from a series of films. Importantly, we demonstrate that the reflectance of HfN across the UV-visible spectrum can be tuned through choice of growth conditions.

The rocksalt structured HfN films were grown on MgO by pulsed laser deposition (PLD). MgO was chosen due to the small lattice mismatch (−7.46%), similar crystal structure, and good thermal match, which allows the growth and study of high-quality films. 1 × 1 cm<sup>2</sup> polished MgO(100) substrates (MaTeck) were bonded to a molybdenum plate using an InSn alloy to provide good thermal contact and loaded into a UHV PLD chamber with a base pressure of 6 × 10<sup>−9</sup> Torr. Film growth was monitored using a Staib re-

flexion high energy electron diffraction (RHEED) system. A 248 nm Lambda Physik KrF laser emitting 25 ns pulses of 80 mJ at 10 Hz was focused on a 99.9% Hf target (Kurt J. Lesker). Laser fluence was maintained constant at (5.0 ± 0.5) J cm<sup>−2</sup> and target to substrate distance was set at 6.0 cm. Substrate temperature was varied in 50 °C steps from 350 to 600 °C to provide a series of films for investigation. Nitrogen was activated using an Oxford Applied Research HD-25 plasma source. Pressure was varied across the range of stable plasma source operating conditions (0.2–1 × 10<sup>−4</sup> Torr), with most samples grown at the upper pressure limit while plasma power was generally set to a stable mid-range value of 200 W. Growth time for all samples was 1 h resulting in films on the order of 100 nm thick, as measured by Rutherford backscattering spectrometry (RBS).

Reflectance of the films was measured using an Ocean Optics fiber-optic spectrometer with a resolution of 0.75 nm full width half maximum. Two mirrors were used as reference sources which between them provided an almost flat reflectance of >99% extending from 488 to 1100 nm. The light source was allowed to warm for several hours before making measurements to ensure consistent light intensity and spectral distribution. Room temperature resistivity and Hall effect measurements were carried out in the Van der Pauw geometry using an EGK Hall effect measurement system with magnetic field of 0.51 T. X-ray absorption and emission spectroscopy (XAS and XES) were undertaken at the nitrogen K-edge using the soft x-ray beamline 511 at MAXlab (Lund, Sweden) which is equipped with a spherical grating monochromator that yielded a resolution of 0.2 eV.<sup>13</sup> XES results were recorded using a Nordgen-type grazing-incidence spherical grating spectrometer with a resolution of 0.3 eV.<sup>14</sup> Absorption data were recorded in fluorescent yield mode with the sample oriented at 75° to the incident beam.

Figure 1 shows RHEED patterns taken along the MgO [100] azimuth before and after growth of a film at 600 °C, using 200 W plasma power and a pressure of 1 × 10<sup>−4</sup> Torr. Kikuchi patterns demonstrate the quality of the substrate surface. Upon commencement of growth, the MgO pattern is replaced by a less-defined HfN pattern. Observation of the

<sup>a)</sup>Electronic mail: ben.ruck@vuw.ac.nz.

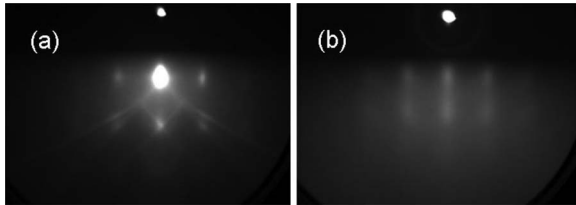


FIG. 1. RHEED patterns from (a) an MgO(100) substrate taken before growth along the [100] azimuth, and (b) post-growth for a film grown at 600 °C.

streak spacing indicates that the lattice is fully relaxed after four min of growth, which corresponds to a thickness of 4–6 nm as measured by RBS. Similar behavior was observed for films grown under other conditions, apart from a sample grown at 400 W plasma power which was polycrystalline. The patterns are quite faint, a common feature we have observed in PLD growth of nitrides from low vapor pressure metal targets; excess metal at the growing surface is not easily desorbed when the substrate temperature ( $\leq 600$  °C) is much lower than the metal desorption temperatures ( $>2000$  °C), which weakens and slightly broadens the RHEED streaks.

Figure 2(a) shows the XES (filled black circles) and XAS (open blue circles) data from a sample grown at

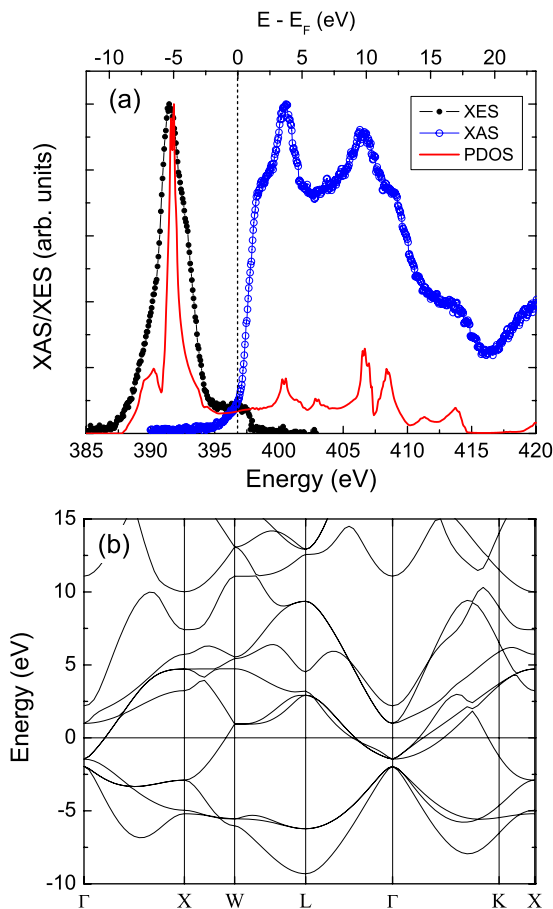


FIG. 2. (Color online) (a) X-ray emission (closed circles) and absorption (open circles) which measure, respectively, the filled and empty nitrogen  $p$ -projected density of states, compared to the calculated PDOS (solid line). The dashed line marks the calculated Fermi level. (b) Calculated band structure of HfN. The bands crossing the Fermi level (0 eV) originate from Hf  $d$ -orbitals.

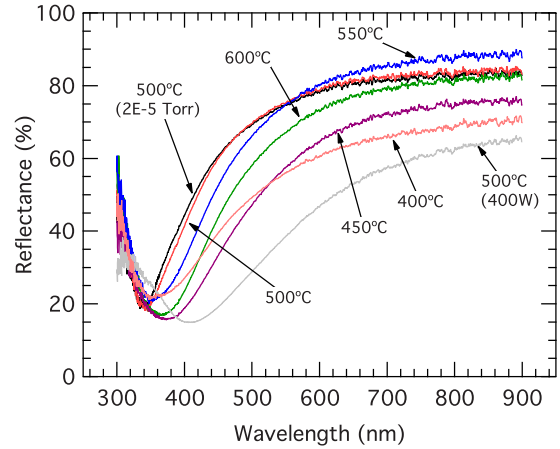


FIG. 3. (Color online) Reflectance spectra for samples grown at various temperatures. Unless indicated otherwise samples were grown under  $1 \times 10^{-4}$  Torr nitrogen, 200 W plasma.

500 °C, 200 W plasma power, and  $10^{-4}$  Torr  $N_2$ , representing the filled and empty N  $p$ -projected partial density of states (PDOS), respectively.<sup>15</sup> We note the overall similarity between the present data and those obtained for rare-earth nitrides, which have the same physical structure and similar electronic configurations.<sup>4</sup> To compare to experiment we have performed a band structure calculation within the local density approximation to density functional theory using the full-potential linearized muffin-tin orbital method.<sup>5,16</sup> The resulting band structure, shown in Fig. 2(b), is similar to that obtained by Stampfl *et al.*<sup>1</sup> The extracted PDOS [red line in Fig. 2(a)] is in excellent agreement with the XAS and XES. Particularly striking is the small but significant density of filled states extending from  $\sim 395$  eV to the Fermi level at  $\sim 397.5$  eV. Such a feature does not occur in semiconducting nitrides. An inspection of the full band structure [Fig. 2(b)] shows that this feature in HfN corresponds to the occupied bands of mostly Hf  $d$  character that cross the Fermi level ( $E_F$ ) and give a small density of states with a weak nitrogen  $p$ -projection. The XAS data appear to overlap slightly with the XES, which we attribute to a small shift of the data due to core-hole effects.<sup>4,17</sup>

As can be seen in Fig. 3, all of the films exhibit a high reflectance across the visible and infrared followed by a rapid decrease in reflectance at short wavelengths and an upturn below about 400 nm, similar to results obtained by Delin *et al.*<sup>8</sup> However, the samples grown with moderate plasma power at temperatures of 500 °C and above have a much higher reflectance which extends further toward the UV than for other samples. This trend does not correlate with surface roughness or particulate density arising from the PLD process, but x-ray diffraction (XRD) results indicate that the more reflective films have the highest crystal quality, with the full-width at half maximum of the  $\theta$ - $2\theta$  [200] reflection equal to  $0.3^\circ$  for the most reflective sample and  $0.6^\circ$  for the least reflective.

XRD measurements place the lattice constant of the better quality samples at around 4.530 Å while for the lower quality samples it is above 4.540 Å. Seo *et al.*<sup>10</sup> found the lattice constant decreases with increasing nitrogen content, and comparison to their data would imply compositions of around HfN<sub>0.95</sub> and HfN<sub>0.8</sub> for the high and low reflectance films, respectively. However, it is interesting to note that

the sample grown under relatively low nitrogen flux ( $2 \times 10^{-5}$  Torr) had one of the highest reflectivities, despite the fact that this sample would be expected to have a relatively high Hf:N ratio. This implies a greater sensitivity to substrate temperature than nitrogen pressure in our HfN growths.

The shape of the reflectance spectra can be addressed in terms of the calculated band structure. The large magnitude of the reflectance across the red and infrared is a direct consequence of the metallic nature of HfN. The roll-off at shorter wavelengths then originates from proximity to the plasma frequency  $\omega_p$ , and the onset of direct band-to-band transitions. The most obvious candidates for the latter occur near  $\Gamma$  from the highest energy portion of the N  $p$ -bands at about  $-2$  eV to the unoccupied Hf  $d$ -bands at approximately 1 eV above  $E_F$ , giving absorption in the energy range  $\sim 3$  eV. Increased disorder reduces the relaxation time, which lowers the reflectance across the visible-IR. This effect is clearly evident in the lower temperature or high plasma power growths. A decrease in  $\omega_p$  also reduces the visible-IR reflectance, as well as moving the position of the reflectance minimum to longer wavelengths.<sup>8</sup> We speculate that variations in carrier concentration induced by changes in stoichiometry may alter  $\omega_p$ , hence explaining the changes in the position of the reflectance minimum between samples.

Room temperature resistivity and Hall effect measurements obtained from the most highly reflecting samples (those grown at 500 °C, 200 W plasma) yielded resistivities between 44 and 75  $\mu\Omega$  cm and mobilities of around 4  $\text{cm}^2 \text{V}^{-1} \text{s}^{-1}$ . The lower resistivity compares reasonably to the minimum reported value for HfN (14.2  $\mu\Omega$  cm),<sup>10,11</sup> and combined with the reflectance data it demonstrates that our HfN films grown above 500 °C are candidates for use as electrical back contacts for light-emitting GaN devices. Temperature dependent data obtained from the film with 75  $\mu\Omega$  cm room temperature resistivity showed only a hint of the onset of superconductivity at 6 K, consistent with the sample being slightly nitrogen poor, in agreement with the XRD and reflectance data.<sup>10</sup>

In summary, epitaxial HfN films have been grown by plasma-assisted PLD on MgO, and their electronic properties

measured across a wide energy range. Films grown at temperatures above 500 °C show larger reflectance which extends further toward the UV, and their electronic structure agrees with the results of a band structure calculation. The fact that the reflectance of HfN can be tuned by varying growth conditions is relevant for optical device applications, for example to optimize light extraction from GaN-based LEDs grown on silicon using a HfN buffer layer.

The research reported here was supported by grants from the New Economy Research Fund (Grant No. VICX0808) and the Marsden Fund (Grant No. 08-VUW-030).

<sup>1</sup>C. Stampfl, W. Mannstadt, R. Asahi, and A. J. Freeman, *Phys. Rev. B* **63**, 155106 (2001).

<sup>2</sup>D. I. Bazhanov, A. A. Knizhnik, A. A. Safonov, A. A. Bagatur'yants, M. W. Stoker, and A. A. Korkin, *J. Appl. Phys.* **97**, 044108 (2005).

<sup>3</sup>E. Zhao and Z. Wu, *J. Solid State Chem.* **181**, 2814 (2008).

<sup>4</sup>A. R. H. Preston, S. Granville, D. H. Housden, B. Ludbrook, B. J. Ruck, H. J. Trodahl, A. Bittar, G. V. M. Williams, J. E. Downes, A. DeMasi, Y. Zhang, K. E. Smith, and W. R. L. Lambrecht, *Phys. Rev. B* **76**, 245120 (2007).

<sup>5</sup>P. Larson, W. R. L. Lambrecht, A. Chantis, and M. van Schilfgaarde, *Phys. Rev. B* **75**, 045114 (2007).

<sup>6</sup>X. Xu, R. Armitage, S. Shinkai, K. Sasaki, C. Kisielowski, and E. R. Weber, *Appl. Phys. Lett.* **86**, 182104 (2005).

<sup>7</sup>R. Armitage, Q. Yang, H. Feick, J. Gebauer, E. R. Weber, S. Shinkai, and K. Sasaki, *Appl. Phys. Lett.* **81**, 1450 (2002).

<sup>8</sup>A. Delin, O. Eriksson, R. Ahuja, B. Johansson, M. S. S. Brooks, T. Gasche, S. Auluck, and J. M. Wills, *Phys. Rev. B* **54**, 1673 (1996).

<sup>9</sup>J. A. Rothschild and M. Eizenberg, *Appl. Phys. Lett.* **94**, 081905 (2009).

<sup>10</sup>H. S. Seo, T.-Y. Lee, I. Petrov, J. E. Greene, and D. Gall, *J. Appl. Phys.* **97**, 083521 (2005).

<sup>11</sup>H. S. Seo, T.-Y. Lee, J. G. Wen, I. Petrov, J. E. Greene, and D. Gall, *J. Appl. Phys.* **96**, 878 (2004).

<sup>12</sup>N. J. Ashley, D. Parfitt, A. Chreneos, and R. W. Grimes, *J. Appl. Phys.* **106**, 083502 (2009).

<sup>13</sup>R. Denecke, P. Vaterlein, M. Bassler, N. Wassdahl, S. Butorin, A. Nilsson, J.-E. Rubensson, J. Nordgren, N. Martensson, and R. Nyholm, *J. Electron Spectrosc. Relat. Phenom.* **101-103**, 971 (1999).

<sup>14</sup>J. Nordgren, G. Bray, S. Cramm, R. Nyholm, J.-E. Rubensson, and N. Wassdahl, *Rev. Sci. Instrum.* **60**, 1690 (1989).

<sup>15</sup>J. Stohr, *NEXAFS Spectroscopy* (Springer, New York, 2003).

<sup>16</sup>H. J. Trodahl, A. R. H. Preston, J. Zhong, B. J. Ruck, N. M. Strickland, C. Mitra, and W. R. L. Lambrecht, *Phys. Rev. B* **76**, 085211 (2007).

<sup>17</sup>U. von Barth and G. Grossmann, *Phys. Rev. B* **25**, 5150 (1982).